Chemical Engineering Journal 114 (2005) 87–97

Chemical Engineering Journal

www.elsevier.com/locate/cej

Kinetics of bacteria disinfection with UV radiation in an absorbing and nutritious medium

Marisol D. Labas, Carlos A. Martín, Alberto E. Cassano *

INTEC, Universidad Nacional del Litoral and CONICET, Güemes 3450, 3000 Santa Fe, Argentina

Received 19 July 2005; received in revised form 23 September 2005; accepted 23 September 2005

Abstract

A kinetic model for water disinfection employing UV-C radiation ($\lambda = 253.7$ nm) was developed that is valid for clear waters as well as for a concentrated and nutritious medium. *Escherichia coli* was used as a test bacteria. The kinetic model is a modification of the series event inactivation mathematical description that takes into account the radiation absorption rate corresponding to the existing, viable bacteria and the radiation attenuation produced by the quasi-transparent or the translucent environment. It also explains two additional observed phenomena: (i) the effect of bacteria growth in the nutritious medium during disinfection and (ii) a further reduction in the inactivation rate that was attributed to some form of bacteria protection produced by a not well understood association of the bacteria with of the components of the concentrated culture. Comparing theoretical predictions from the model with experimental concentration versus time data, the model parameters were obtained. Predictions show good agreement with collected experimental data within the range of the explored variables.

Keywords: Water disinfection; Ultraviolet radiation; *Escherichia coli*; Photoreaction model

1. Introduction

The use of UV-C radiation (wavelengths between 180/200 and 280 nm) for water disinfection is a well-known and effective application for an ample group of microorganisms providing a reliable and simple technology. It is particularly attractive due to the absence of undesirable secondary effects usually found in several classic chemical treatments, such as the generation of disinfection byproducts (DBPs) or a change in the organoleptic properties of the treated water [1–3]. Within this context several advanced oxidation processes (AOP) employing UV alone or in combination with hydrogen peroxide, ozone or semiconductor catalysts have been proposed [4]. The ability of short wavelength UV radiation to treat secondary effluents from sewage disposal plants has been summarized by Blatchley and Scheible [5] and a revision of its application in the food industry has been recently made [6].

The UV-C radiation emission spectrum, particularly the one produced by commercially known as germicidal lamps (90% plus emission at $\lambda = 253.7$ nm) has an important overlapping with the absorption peak of DNA and it is believed that its effect on microorganisms is a significant change in the DNA structure, producing a pyridine dimerization that has lethal consequences [7].

Since the first proposal of a kinetic model for chemical water disinfection by Chick [8] several modifications have been introduced to improve the applicability of the resulting mathematical descriptions to explain different process features. However, the first specific modeling contribution concerning the use of UV radiation can only be traced back to the work of Severin [9] with the proposal of two different approaches: the multi hit and the series event models. Both derived expressions were able to explain the anomalous behavior at the initial stages of disinfection in a concentration versus time representation of the inactivation process. Oliver and Cosgrove [10] observed that anything in the water that absorbs radiation or shields the bacteria from the UV light would be expected to influence the rate of bacteria kill. Emerick et al. [11] also observed some sort of resistance to the UV attack for long inactivation times. The existence of some form of bacteria protection (for example, agglomeration, shielding by existing solid particles or bacteria association with some components of the medium) was proposed to explain this phenomenon that manifests as a long tailing in a plot of the bacteria concentration versus the inactivation time and gives rise

* Corresponding author. Fax: +54 342 4559185.
E-mail address: acassano@ceride.gov.ar (A.E. Cassano).

1385-8947/$ – see front matter © 2005 Elsevier B.V. All rights reserved.
doi:10.1016/j.cej.2005.09.013

Nomenclature

$C_{Ec,i}$	*Escherichia coli* concentration of species with state of damage i (CFU cm^{-3})
C_m	medium concentration (g cm^{-3})
CFU	colony forming units
e^a	local volumetric rate of photons absorption (LVRPA) W cm^{-3} or (einstein cm^{-3} s^{-1})
G	incident radiation W cm^{-2} or (einstein s^{-1} cm^{-2})
k	inactivation kinetic constant (s^{-1} (cm^3 s einstein^{-1})^m or s^{-1} (cm^3 W^{-1})^m)
k_G	growth constant (CFU g^{-1} s^{-1})
k_{obs}	observed constant
k_{prot}	protection constant
L_R	reactor length (cm)
m	reaction order with respect to e^a
n	threshold limit of damage
$R_{Ec,i}$	reaction rate corresponding to the bacteria with a state of damage i (CFU cm^{-3} s^{-1})
R_G	growth rate (CFU cm^{-3} s^{-1})
R_i	reaction rate of component i (mol cm^{-3} s^{-1})
R_P	protecting rate (CFU cm^{-3} s^{-1})
t	time (s)
V	volume (cm^3)
x	Cartesian coordinate along the reactor length (cm)
$\underline{x}$	position vector (cm)

Greek letters

$\alpha_{Ec,i}$	*E. coli* specific Napierian absorption coefficient (cm^2 CFU^{-1})
α_m	medium specific Napierian absorption coefficient (cm^2 g^{-1})
κ	Napierian absorption coefficient (cm^{-1})
λ	wavelength (nm)
Φ_i	quantum yield of component i (mol einstein^{-1} or molecule quanta^{-1})
Φ_{Inact}	pseudo-quantum yield for bacteria disinfection (CFU quanta^{-1})

Subscripts

Ec	relative to *E. coli*
i	relative to the damaging state i or to the species with a damaging level i
R	relative to reactor
T	relative to total
W	relative to reactor wall
0	denotes initial value
λ	relative to wavelength

Special symbols

$\langle\cdot\rangle$	means averaged value
[=]	means "has units of"

to great difficulties in reaching an acceptable disinfection level in the treated water [10,12–17].

Most of the reactor designs employed in AOP are made with empirically adjusted models having different parameters that vary according to the apparatus and the particular effluent that is treated. Very often the performance of such units is rated with approximate indicators based on the operating conditions such as, for example, the "electrical energy per order" [4] that relates the energy consumption with one order of magnitude decrease in pollutant concentration. On the other hand, other authors [18] are inclined to use more deterministic models derived from reactor engineering fundamentals, describing, when necessary, the motion of the fluid and its consequences on the distribution of residence times as well as the spatial distribution of radiation employing the radiative transfer equation (RTE) and, finally, incorporating all this information in the mass balances with the corresponding kinetic models. In these expressions the different features affecting the disinfection rates should be taken into account (photoprotection, aggregation, association, etc.) specially if some of these phenomena can be enhanced by the characteristics of the effluent to be treated that could have suspended solids [19,20] or nutritious substances as it is the case of this work. Of particular interest is the model developed by Emerick et al. [21] that describe the existence of two parallel processes: (i) the inactivation of dispersed bacteria that follows a first order rate with respect to the surviving bacteria exposed to an average value of the incident radiation in the bulk of the solution and (ii) the inactivation of particle-associated bacteria that is described in terms of a parameter that accounts for the fraction (between 1 and 0) of the light that reaches this special group of microorganisms. This parameter presents a distribution from 1 for microorganisms with direct exposure to the averaged light intensity and 0 for microorganisms located in a completely shielded region. The model of this second process is made in terms of a sum over the distribution of the shielding parameter and a classical first order inactivation rate. The concentration of particles must be known and it was shown that for each type or microorganism a minimum critical size of the particle is required to produce the shielding effect [17,20].

Labas et al. [22] developed a kinetic model for UV disinfection under almost clear water conditions contaminated with *Escherichia coli* based on a modification of Severin's series event description. This type of environment corresponds to the "disperse bacteria" group in Emerick et al. [21] modeling approach. The collected experimental information was in full agreement with the mathematical model. The present work is an extension of the previous one attempting to represent additional phenomena observed when the process was not performed in almost transparent waters as well as in absence of nutritious substances. With the relevant exception of water treatment for domestic use or equivalent applications, the situation described in this work is closer to many applications concerning industrial effluents. Consequently, in this work, besides the requirement of a precise description of the spatial distribution of the radiation field originated in a much higher medium optical thickness, two additional phenomena could be present and must be accounted for: (i) the possibility of bacteria growth and (ii) the possibil-

ity of bacteria protection resulting from some sort of defensive effect produced by the concentrated medium. In what follows a model is presented to mathematically describe this performance that could be encountered in some treatment plants having effluents containing nutritious substances. It is proposed that this extension should be also able to represent the case of almost transparent waters. Summarizing this introduction, the main objective of this contribution is to obtain a kinetic model that could be used for scaling up purposes in some disinfection processes and is described in terms of plausible assumptions and easily observable variables.

2. The reacting system

In order to write the appropriate and certainly very special kind of "mass" balance the experimental reactor must be described. It is shown in Fig. 1 and the most salient data are presented in Table 1. The reactor is a Pyrex tube of circular cross-section having two parallel, flat windows made of Suprasil quartz. Each window is irradiated by an emission system made of a tubular low-pressure mercury lamp (germicidal type) placed at the focal axis of a parabolic reflector. With the proper dimensions and geometric layout this system produces a very good approximation to a one dimensional radiation field [23] facilitating the description of the radiation distribution inside the reactor. No radiation can reach the reactor from the cylindrical wall; moreover, Pyrex glass is almost opaque to germicidal lamps ($\lambda = 253.7$ nm). Two different types of radiation sources were used: (i) two Philips TUV lamps having a nominal input power of 15 W each and (ii) two Heraeus NNI40 UV-C lamps operated with a nominal input power of 40 W each. They are low-pressure mercury vapor lamps (Germicidal type) with one single, significant emission wavelength at 253.7 nm. Each reactor window permitted the interposing of: (1) one shutter to block the passage of light when desired (for example, to allow for the lamp to reach its steady state operation) and (2) neutral density filters to vary the irradiation rate from the lamps and reflectors permitting, with this device, two additional irradiation rates (four in total).

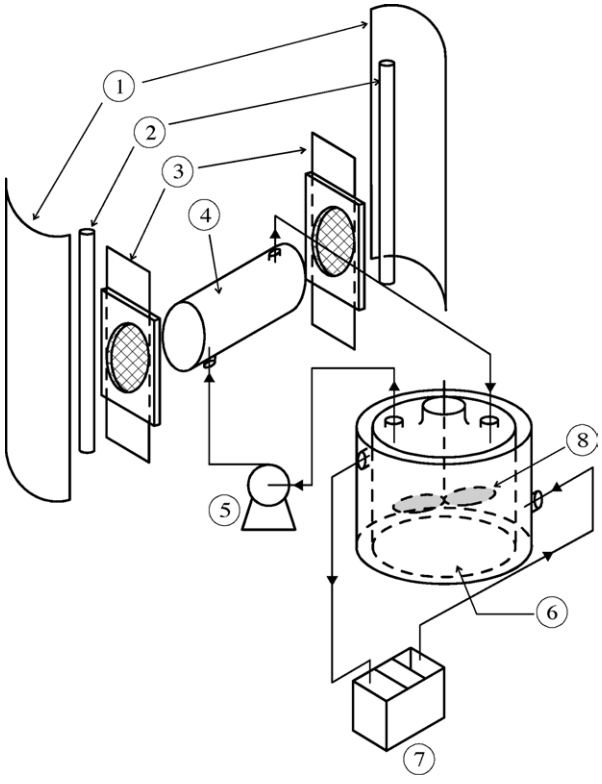

Fig. 1. Experimental set up. (1) Parabolic reflectors, (2) lamps, (3) filters, (4) photoreactor, (5) pump, (6) tank, (7) thermostatic bath and (8) stirrer.

Table 1
Reactor characteristics (experimental apparatus)

Reactor (quartz windows)	
Length	4.9 cm
Diameter	4.4 cm
Volume	74.5 cm^3
Storage tank (Pyrex)	
Volume	1000 cm^3
Lamps (output power (253.7 nm))	
Heraeus NNI40	16 W
Philips TUV15	3.5 W
Reflectors	
Parabolic	Aluminum with Alzac treatment
Pump	
Masterflex flowrate	35 $cm^3\ s^{-1}$

The reactor was placed inside a recirculating system that includes a pump (Masterflex 7553-76) and a well-stirred storage tank with provisions for sampling and temperature control. Good mixing in the reactor was achieved, by means of an intense recirculation of the liquid. It can be shown [24] that under some well defined operating conditions, this experimental device operates as a special type of well-mixed batch reactor having only a fraction of its total volume ($V_R/V_T \ll 1$) exposed to irradiation producing an artificial prolongation of the reaction time that greatly facilitates sampling at the initial stages of the inactivation process. The liquid in the tank was kept at constant temperature (20 °C) by means of a jacket connected to a recirculating water thermostatic bath (HAAKE). Connections between the different components of the recycle were achieved with silicone tubing. This reactor set up was build for laboratory research and under no circumstances must be regarded as a proposal for industrial applications.

3. The experimental procedure

E. coli strain ATCC 8739 was used throughout this work. The culture was grown in two different types of broth: (i) A complex medium (nutrient broth) having as main component beef extract and (ii) a synthetic medium of well-known composition having as main component glucose. In the first case the broth composition was—tryptone: 10 g L^{-1}, beef extract: 5 g L^{-1} and NaCl 5 g L^{-1}. In the second case the broth was prepared according to the components and concentrations suggested by Bailey and Ollis [25]. The working solution was prepared from a culture that had reached the stationary phase of growth (always ca. 10^8 colony forming units per cm^3) and, afterwards, brought to the

Table 2
Operating conditions and optical properties of the components

Operating conditions	
Initial conditions	
Escherichia coli C^0_{Ec}	10^4 to 10^8 CFU cm^{-3}
Medium (C_m)	10^{-3} to 10^{-6} g cm^{-3}
Average residence time per pass in the photoreactor	2.1 s
Ratio of V_R/V_T	0.07
Optical characterization	
Specific absorption coefficients of the reacting medium components (α_i) at 253.7 nm	
E. coli	1.38×10^{-9} cm^2 CFU^{-1}
Nutrient broth	1284 cm^2 g^{-1}
Glucose broth	144 cm^2 g^{-1}

desired dilution with sterilized saline. Concentration of oxygen (air) and temperature (20 °C) were kept constant.

The specific absorption coefficients (Napierian absorptivities) of the two different culture media and *E. coli* were measured in a UV–vis Lamda 40 Perkin-Elmer Spectrophotometer at 253.7 nm. The results are shown in Table 2. In a previous work [22] it was shown that all the cultures behave as a homogenous system having absorbances that show a linear dependence with the species concentration. Most of the initial *E. coli* CFU concentrations ranged from 10^4 to 10^7 CFU cm^{-3} depending upon the dilution of the culture, but some runs were also made with values above $C^0_{Ec} = 10^8$ CFU cm^{-3}.

The lamps were turned on, allowing for 30 min to stabilize their operation (during this time the shutters at the reactor windows were on). The working solution was added to the reactor. Immediately after, recirculation was established until the temperature gave a constant reading. All inactivation runs were made under isothermal conditions at 20 °C. The sample at $t = 0$ was taken at the same time that the lamp shutters were taken off. Afterwards, samples were taken at different time intervals for several measurements. After every run the whole equipment was carefully disinfected with sodium hypochlorite dilute solution, followed by dilute ethanol solution and several washing operations with distilled water. Runs were always duplicated in order to ensure reproducible results and minimize errors.

Samples were taken initially every 10 s and, afterwards, during the first 600 s every 60 s. A normal run lasted from 1000 to approximately 12,000 s depending on the operating conditions. Dilution of the samples to obtain the optimum concentration for the CFU counting method was made with sterile peptone water solution. Triplicate measurements of all samples were made. Each sample was subjected to the following measurements: absorbance at 253.7 nm and CFU counting using specific Petrifilm™ plates (3 M Microbiology Products) for *E. coli* and coliform bacteria. The limit of detectable bacteria for enumeration was 15 CFU cm^{-3} when the sample of 1 cm^3 was plated directly.

4. Modeling equations for almost clear water conditions

The starting point for the modeling of the present research is a set of equations already derived in previous work [22,24,26]. These expressions will give the upper limit of the inactivation rates considering that all of the microorganisms are fully dispersed. They were obtained in the following sequence:

(i) Inactivation is considered a special type of reaction resulting from the interaction of the UV radiation with some of the chemical components of the bacteria.

(ii) The inactivation reaction is modeled with a modification of the series event approach and represented by a set of successive reactions called damaging reactions according to the state of damage "*i*" that the microorganism has been subjected to ($i = 0, 1, 2, \ldots, n$). n is the threshold limit of damage when the bacteria become inactivated. The details of the derivation were described in Labas et al. [22] and the results are:

$$R_{Ec,i}(\underline{x}, t) = \begin{cases} -kC_{Ec,i}[e^a_{Ec,i}(\underline{x}, t)]^m + R_G & \text{for } i = 0 \\ kC_{Ec,i-1}[e^a_{Ec,i}(\underline{x}, t)]^m - kC_{Ec,i}[e^a_{Ec,i}(\underline{x}, t)]^m + R_G & \text{for } i = 1, \ldots, n-1 \\ kC_{Ec,i-1}[e^a_{Ec,i-1}(\underline{x}, t)]^m & \text{for } i = n \end{cases} \quad (1)$$

Essentially, the rate has a linear dependence with respect to the viable bacteria concentration and is also proportional to the radiation absorption rate by the viable bacteria risen to an unknown order (m). This means that the effect of the light intensity is not assumed to be of first order and, additionally, the relationship is established in terms of the absorbed intensities. This assumption is in accordance with the experimental evidences reported by Oliver and Cosgrove [10] that indicated that the inactivation rate does not show a linear relationship with the applied light intensity.

(iii) A series of damaging events are needed to reach the point of bacteria inactivation. The threshold limit of events (n) is an additional parameter of the model.

(iv) As indicated in (ii) the inactivation rate is a function of the UV radiation energy absorbed by the bacteria. The available energy for absorption is a function of: (1) the medium concentration, (2) the time dependent radiation absorption produced by the variation of viable *E. coli* concentration and (3) the position inside the reactor, particularly due to the radiation attenuation in a non-transparent media. Thus, in order to know the existing radiation field as a function of position and time, the radiative transfer equation (RTE) must be solved inside the reactor. For one dimensional irradiation, valid for the employed experimental device, the resulting equations are:

$$G(x, t) = G_w\{\exp[-\kappa_T(t)x] + \exp[-(\kappa_T(t)x)(L_R - x)]\} \quad (2)$$

Table 3
Boundary conditions (G_w; from actinometric measurements) of the reacting system [22]

Experimental conditions	
Heraeus NNI40	14.95×10^{-9} einstein cm^{-2} s^{-1}
With neutral density filter (17%)	2.55×10^{-9} einstein cm^{-2} s^{-1}
Philips TUV15	5.85×10^{-9} einstein cm^{-2} s^{-1}
With neutral density filter (17%)	0.97×10^{-9} einstein cm^{-2} s^{-1}

$$\kappa_T(t) = \sum_{i=0}^{n-1} \kappa_{Ec,i}(t) + \kappa_m = \sum_{i=0}^{n-1} \alpha_{Ec,i} C_{Ec,i}(t) + \alpha_m C_m \quad (3)$$

$$e^a_{Ec,i} = \kappa_{Ec,i}(t) G(x,t) \quad (4)$$

Note that a different type of reactor will require the use of the appropriate and very likely different form of the RTE that, in the most general case, is a three-dimensional equation.

(v) The solution of the RTE requires the knowledge of a boundary condition: the incident radiation at each reactor window: G_w. It was experimentally obtained with chemical actinometry resorting to an interpretation of the results according to the description made in Labas et al. [22]. The results are shown in Table 3.

(vi) The reaction rates are incorporated into a special type of "mass" balance in terms of the colony forming units (CFU) concentrations. The final equation is

$$\left.\frac{dC_{Ec,i}(t)}{dt}\right|_{T_k} = \frac{V_R}{V_T} \langle R_{Ec,i}(x,t) \rangle_{V_R} \quad (5)$$

with

$$t = 0 \begin{cases} i = 0 & C_{Ec,0} = C^0_{Ec,0} \\ i = 1, \ldots, n & C_{Ec,i} = 0 \end{cases} \quad (6)$$

and

$$\langle R_{Ec,i}(x,t) \rangle_{V_R} = \frac{1}{V_R} \int_{V_R} R_{Ec,i}(x,t)\, dV = R_{Ec,i}(t) \quad (7)$$

The derivation for an analogous experimental device can be found in Labas et al. [24]. However, it must be clearly stated that this equation is valid when: (i) the reactor and the tank are well mixed, (ii) the recirculation rate is high, (iii) $V_R/V_T \ll 1$ and (iv) the change in concentration per pass in the reactor is rather small (which results from the mentioned high recirculation flowrate). Notice that the ratio of V_R/V_T is explicitly shown in the CFU balance and that the changes in concentration are measured in the tank. It must be also clearly noted that since the inactivation rates are a function of position through their direct dependence with the local value of the radiation absorption rate by the viable bacteria, they must be reactor volume averaged before integrating the CFU balances. For a well-mixed reactor this averaging procedure strictly applies to the radiation field.

These equations must be solved numerically because the CFU balances and the radiation transport equation are coupled through the variable bacteria concentration along the reaction time t. Consequently, iteration is unavoidable. The final result from the theoretical model is a set of pairs of values of CFU concentrations versus time. These results can be compared with the same pairs of experimental information collected in the reactor employing a non-linear, multiparameter estimator assisted with an optimization program. The results of this parameter estimation are: (1) the average number of damaging steps needed for inactivation (n) that is forced to be an integer, (2) the inactivation kinetic constant (k), and (3) the reaction order with respect to the radiation absorption rate (m). The kinetic constant for the growing reaction k_G can be obtained with separate experiments.

Typical results under almost clear water conditions [water practically transparent to the UV irradiation prepared with a large dilution (1/1000) of the original culture medium] are shown in Fig. 2(a). It is a plot of the changes in *E. coli* concentration (in terms of colony forming units) as a function of time resulting from averaged duplicated runs and triplicate Petrifilm™ sample measurements. These conditions could be assimilated to the case of a plant treatment for domestic distribution of potable water. The obtained inactivation is at least 99.99% in rather short contact times. It must be noted that the ratio of V_R/V_T is 0.07 and, consequently, the effective contact times are more

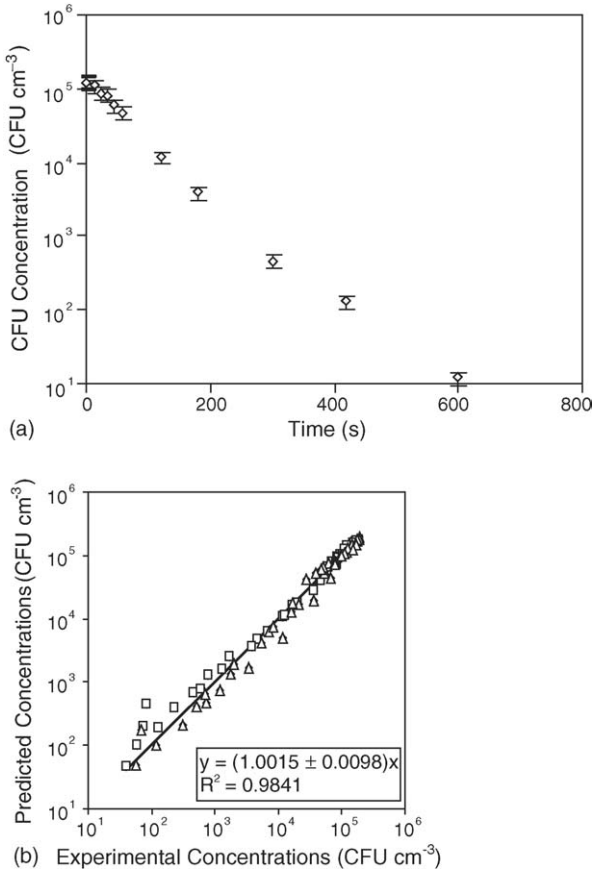

Fig. 2. (a) Typical experimental data of bacteria inactivation corresponding to the transparent, diluted medium. $C^0_{Ec} = 1.25 \times 10^5$ CFU cm^{-3}; $C_m = 5 \times 10^{-6}$ g cm^{-3} and Philips TUV15 lamp (100%). (b) Comparison of model predictions vs. experimental data of bacteria inactivation corresponding to diluted medium [Eqs. (1)–(7)]: (□) bacteria grown with the synthetic medium, (△) bacteria grown with nutrient broth. Runs were made with Heraeus NNI40 lamps (100% and 17% input power) and Philips TUV15 lamps (100% and 17% input power).

than 14 times shorter. For this case, Labas et al. [22] model have shown an excellent agreement between theoretical predictions [according to Eqs. (1)–(7)] and experimental values as shown in Fig. 2(b) for an ample range of the explored variables (different irradiation rates, initial CFU concentrations and two different diluted media: synthetic medium and nutrient broth). In all the experiments the reacting medium was diluted and under these conditions it was found that $R_G \cong 0$. With a 95% confidence interval, the estimated parameters including both media were: $n = 2$, $m = 0.205 \pm 0.015$, $k = 9.03 \pm 0.36$ $(\text{cm}^3\,\text{W}^{-1})^m\,\text{s}^{-1}$ or $k = 1.31 \times 10^2 \pm 5.21$ $(\text{cm}^3\,\text{s einstein}^{-1})^m\,\text{s}^{-1}$.

5. Preliminary experiments with a strongly absorbing and nutritious medium

Fig. 3 presents a typical result of the average of two duplicated inactivation runs in the concentrated medium processed according to the previously described procedure. A tailing on the plot of CFU concentration versus time is clearly observed. It is equally evident that Eqs. (1)–(7) with $R_G \cong 0$ will not represent this performance. This tailing phenomenon has been reported previously by several authors, for example Oliver and Cosgrove [10], Emerick et al. [11], Qualls et al. [12], Loge et al. [16], and Taghipour [20] as well as others already mentioned in Section 1.

It is clear that the photon concentration profiles (the distribution of the available energy as a function of the reactor length) under the new operating conditions must be quite different. However, the change in the attenuation of the radiation field due to the existence of a much more concentrated medium is taken into account by the radiation transport equation. In effect, the total absorption coefficient, calculated according to the corresponding (in this case, very different) optical properties of the reaction space, is part of the model described by Eqs. (2)–(4). Fig. 4 shows the different values of the local volumetric rate of photon absorption by the bacteria (at initial conditions) when concentrated and dilute media are used. For a better understanding of the observed differences, Fig. 5 shows the same properties for the two different cultures (concentrated and diluted conditions). All the plots show the change in the radiation absorption

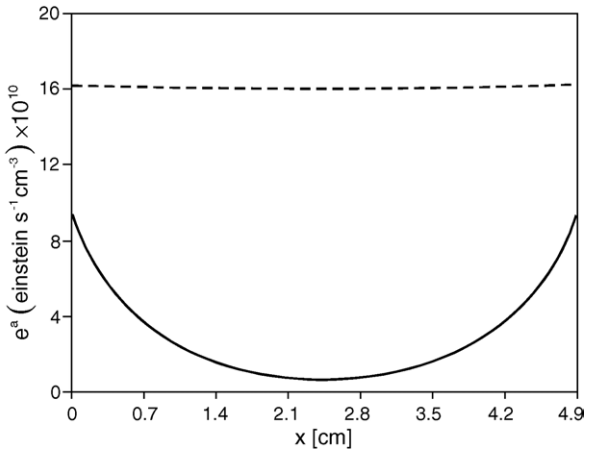

Fig. 4. Bacteria local volumetric rate of photon absorption distribution inside the reactor at initial conditions. $C^0_{Ec} = 4.5 \times 10^7$. Solid line: using nutrient broth with $C_m = 1 \times 10^{-3}$ g cm^{-3}; broken line: using synthetic broth with $C_m = 5 \times 10^{-6}$ g cm^{-3}. $G_w = 14.95 \times 10^{-9}$ einstein cm^{-2} s^{-1}.

rate by the bacteria (at the same initial concentrations) or by the media as a function of the distance from the windows of radiation entrance. Therefore, as indicated by Eqs. (2)–(4), the exponential attenuation will have a very important effect. This change is irreducible because of the large differences in the characteristic times corresponding to mixing and photon transport. Thus, the model uses the irradiation rate at the reactor window (the incident radiation G_w) only as a boundary condition for the RTE, but takes fully into account the existence of a stronger radiation absorbing medium (the concentrated culture) when the value of κ_m is incorporated into $\kappa_T(t)$. These differences in the available energy as a function of the position along the reactor length (the incident radiation distribution in the reaction space), producing a whole field of different inactivation rates as a function of the spatial position, have been taken into account by Eqs. (2)–(4) and cannot explain the observed phenomena (the tailing effect). Notice once again that the calculated rates are the result of volume-averaged values to take into account the fact that experimentally measured values represent the result of bacteria exposed to different irradiating conditions produced

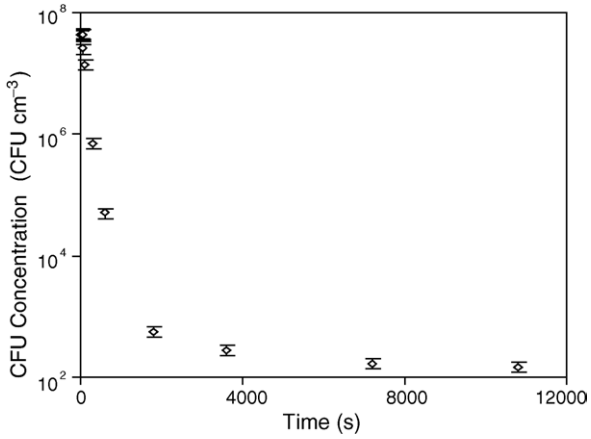

Fig. 3. Typical experimental data of bacteria inactivation corresponding to the concentrated medium.$C^0_{Ec} = 6.9 \times 10^7$ CFU cm^{-3}; nutrient broth with $C_m = 1 \times 10^{-3}$ g cm^{-3} and Philips TUV15 lamp (100%).

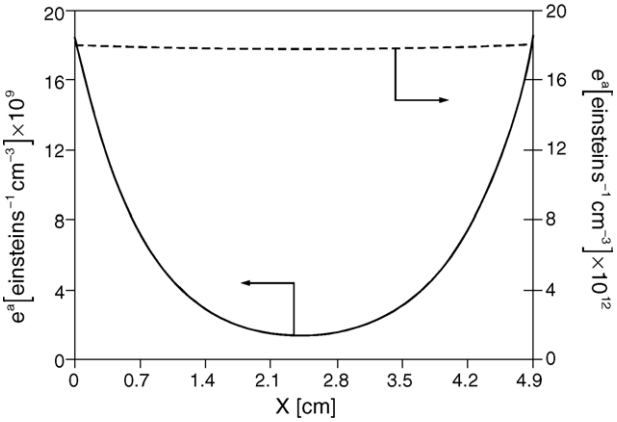

Fig. 5. Medium local volumetric rate of photon absorption inside the reactor at initial conditions. Solid line: $C_m = 1 \times 10^{-3}$ g cm^{-3}; broken line: $C_m = 5 \times 10^{-6}$ g cm^{-3}. $C^0_{Ec} = 4.5 \times 10^7$. $G_w = 14.95 \times 10^{-9}$ einstein cm^{-2} s^{-1}.

by the operating conditions of mixing. In conclusion, the radiation attenuation effect produced by the concentrated medium is explicitly considered in the employed radiation model and a phenomenological correction as suggested by Loge et al. [16] to account for this change is not compatible with this model.

The possibility that the concentrated medium may significantly change its optical characteristics during the run should be analyzed. The following experiment was performed in order to investigate the invariance of the optical properties of the media employed to carry out the inactivation reaction when they were exposed to germicidal lamp irradiation. The employed concentrated media, without bacteria, were irradiated during more than 1 h (3800 s). In both cases, the observed changes in absorbance were always within the experimental error. In any event, the same measurement was made for every sample in order to use in each case the corresponding radiation absorption characteristics.

Experiments were also carried out to observe the possibility that UV-induced genetic flaws could result in population heterogeneity and high resistance to UV irradiation among a small fraction of bacteria in the existing population. Starting with a CFU concentration in the order of 10^7 CFU cm^{-3}, runs were made during approximately 12,000 s under the normal operating conditions. During this run, at $t = 2000$ s samples were taken having a CFU concentration in the order of 10^2 CFU cm^{-3}. Employing the bacteria of these samples (taken at $t = 2000$ s), the normal protocol was followed to grow a new culture up to a concentration in the order of 10^7 CFU cm^{-3}. With the culture prepared with the daughter bacteria, inactivation runs were performed again during approximately 12,000 s under the same experimental conditions than with the mother culture. The results are shown in Fig. 6.

No significant differences were observed between the behavior of the mother culture and that of the daughter one. The tailing and the plateau are similar in both cases. One can conclude that from the inactivation kinetics point of view both cultures have the same response. In other words, the development of a more resistant colony to UV irradiation cannot be deduced from the kinetic response of the daughter culture. One can say that from the kinetic point of view – and exclusively based on this limited observation – UV radiation does not seem to induce a significant change in the characteristics of the surviving, viable bacteria.

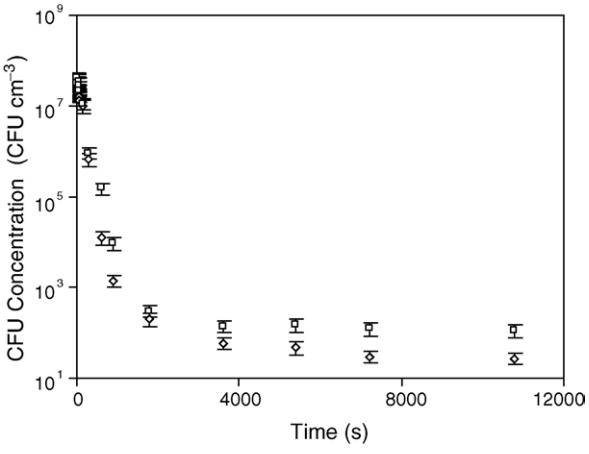

Fig. 6. Comparison of UV inactivation of "mother" and "daughter" cultures of *Escherichia coli*: (□) "mother culture", $C^0_{Ec} = 4 \times 10^7$ CFU cm^{-3}; (◊) "daughter culture", $C^0_{Ec} = 2.5 \times 10^7$ CFU cm^{-3}; nutrient broth with $C_m = 1 \times 10^{-3}$ g cm^{-3} and Heraeus NNI40 lamp (100%). All bacteria were grown with nutrient broth.

6. A model for a concentrated nutritious medium

6.1. The growing effect

When the reaction environment contains nutritious components the possibility that the fraction of viable bacteria (not yet inactivated) continue with its reproductive activity at an appreciable rate cannot be disregarded. This also includes those microorganisms that may have been subjected to partial damage only and are not totally inactivated. In order to analyze this possibility, the following set of experiments was carried out: The inactivation reaction was performed during approximately 2000 s and immediately after the UV lamps were turned off. Maintaining the recirculation in the recycling system the experiment was continued during approximately 6000 additional seconds in the dark. It was observed a growth in the concentration of CFU as it is shown in Fig. 7. It can be noted that the previously shown plateau in Fig. 3 has been substituted by a moderate increase in the *E. coli* concentration. This type of run was repeated employing different medium concentrations and starting the dark experiments with different CFU concentrations. The results of a typical experiment are depicted in Fig. 8 where a clear linear dependence of a pseudo-growing constant with respect to the medium concentration is shown. It is very important to note that, under these experimental conditions, the rate of growth was independent of the bacteria concentration; i.e., the observed rate was of zero order with respect to the CFU concentration. This very unusual behavior has been observed before and interpreted as the resulting effect of the stress and partial damage that the bacteria have been subjected to during the time that they have been exposed to the UV radiation [27]. An additional cause cannot be neglected: the concentration of some of the indispensable components of the medium could have been seriously depleted during the standard growing protocol.

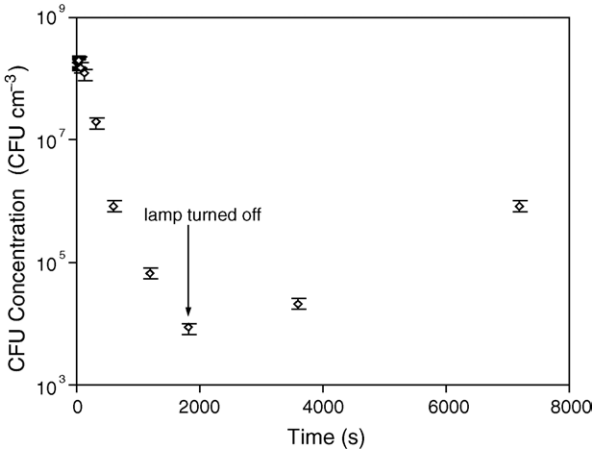

Fig. 7. Bacterial growth in the system after the lamp was turned off. $C^0_{Ec} = 1.89 \times 10^8$ CFU cm^{-3}; nutrient broth with $C_m = 4 \times 10^{-3}$ g cm^{-3} and Heraeus NNI40 lamp (100%).

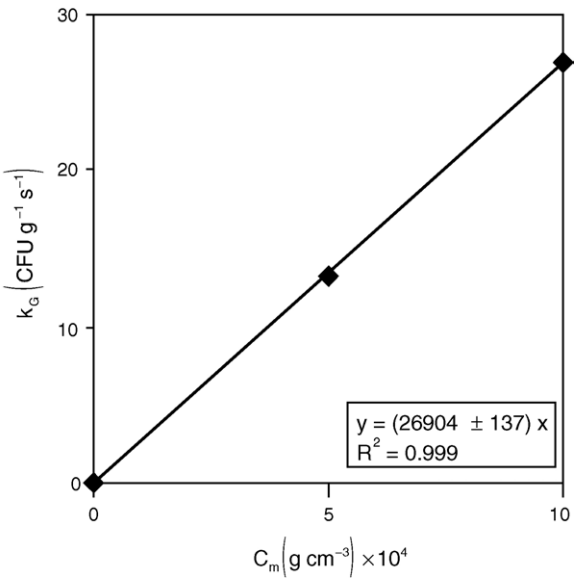

Fig. 8. An example of the growth constant dependence with respect to C_m.

It must be specially noted that growing experiments carried out with non-irradiated bacteria and fresh culture, have shown the typical Michaelis–Menten growth. The rate of growth was modeled with a very simple expression representing a first order dependence with respect to the medium concentration:

$$R_G = k_G C_m \quad \text{for } i = 0,\ 1, \ldots, n-1 \tag{8}$$

Differing from the case corresponding to almost transparent water (where the nutritious components concentrations were negligible and it was found that $R_G = 0$) it seems reasonable that Eq. (8) must be incorporated into the model equations. Note that this "reaction" takes place in the whole system (V_T) while inactivation only occurs in V_R. There is no doubt that the observation of this phenomenon was facilitated by the employed experimental device (the recirculating system with the large volume storage tank). The growing rate is not too large; therefore it becomes comparable with the inactivation rate (which exhibits a strong dependence on the CFU concentration) when the bacteria concentration is rather low; i.e., when the exposition time is large, both rates may be of similar order of magnitude and the combination of both effects seems to be partially responsible for the observed plateau. In conclusion, in concentrated, nutritious media bacteria growth may give rise to a competitive effect that precludes the possibility of reaching negligible concentrations of bacteria inactivation. In any event it is fair to note that a damage-repair mechanism in the dark, with a similar kinetic behavior, cannot be totally excluded.

In order to have a quantitative evaluation of the significance of this growing rate the following information was calculated. The initial reaction rate (just after the very few seconds of induction time) was compared with the growing rate employing the same culture. The growing rate is eight orders of magnitude smaller that the initial inactivation rate. They become comparable only after 3600 s of irradiation when the concentration of viable bacteria has been drastically diminished.

6.2. The association effect

The observed experimental information also suggested that some form of protection beyond the significant attenuation in the radiation field is taking place. The inactivation rate with the concentrated medium is different as it can be deduced from the slope of the plots of CFU concentration versus time. The reasons for this additional reduction in the inactivation reaction are not clear. The phenomenon takes the appearance of some form of bacteria protection by some of the components of the nutritious medium. Notwithstanding that a similar behavior has been observed by others, in most cases the reported shielding effect have been almost always associated with the presence of solid particles [11,12,19,20]. One could hypothesize, and this is an assumption of the model, that this sort of protection is related with the medium concentration (recall that in this work, particles were not present). The first and simpler approximation is to assume a first order dependence. Eq. (1) represents the maximum inactivation rate for totally "dispersed" bacteria. Then, it is proposed to complete the model subtracting from the equation describing the inactivation in a medium of totally dispersed bacteria, the fraction that is being protected by some sort of association with the components al the concentrated culture:

$$R_P(x,t) = \begin{cases} (k_{prot}C_m)C_{Ec,i}[e^a_{Ec,i}(x,t)]^m & \text{for } i = 0 \\ (k_{prot}C_m)C_{Ec,i-1}[e^a_{Ec,i-1}(x,t)]^m + (k_{prot}C_m)C_{Ec,i}[e^a_{Ec,i}(x,t)]^m & \text{for } i = 1,\ldots,n-1 \\ (k_{prot}C_m)C_{Ec,i-1}[e^a_{Ec,i-1}(x,t)]^m & \text{for } i = n \end{cases} \tag{9}$$

In Emerick et al. [21] conceptual description for a medium with particles of different size these equations represent the group of "associated" bacteria that do not receive the incident radiation corresponding to the radiation distribution field described by Eqs. (2)–(4). Diffusion limitations have not been considered to explain this phenomenon because of the prevailing very strong mixing conditions. Moreover, no mass transfer limitations were observed when the inactivation rates were very high and this effect could have been of greater significance.

7. Final equations

Eqs. (8) and (9) can be incorporated in the set of equations derived for the almost transparent medium. The result is

$$R_{Ec,i}(x,t) = \begin{cases} -(k - k_{prot}C_m)C_{Ec,i}[e^a_{Ec,i}(x,t)]^m + k_G C_m & \text{for } i = 0 \\ (k - k_{prot}C_m)C_{Ec,i-1}[e^a_{Ec,i-1}(x,t)]^m - (k - k_{prot}C_m)C_{Ec,i}[e^a_{Ec,i}(x,t)]^m + k_G C_m & \text{for } i = 1,\ldots,n-1 \\ (k - k_{prot}C_m)C_{Ec,i-1}[e^a_{Ec,i-1}(x,t)]^m & \text{for } i = n \end{cases} \tag{10}$$

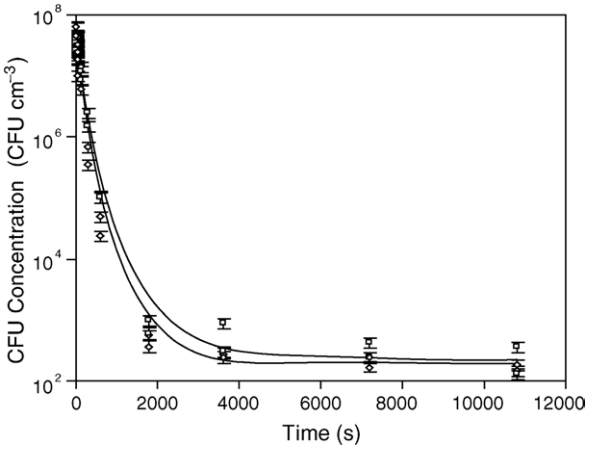

Fig. 9. Comparison of model predictions and experimental data of bacteria inactivation. Solid lines: model predictions; experimental data: (◊) Heraeus NN40I lamp; (□) Philips TUV15 lamp; nutrient broth with $C_m = 1 \times 10^{-3}$ g cm^{-3} and $C^0_{Ec} \cong 10^7$ CFU cm^{-3}.

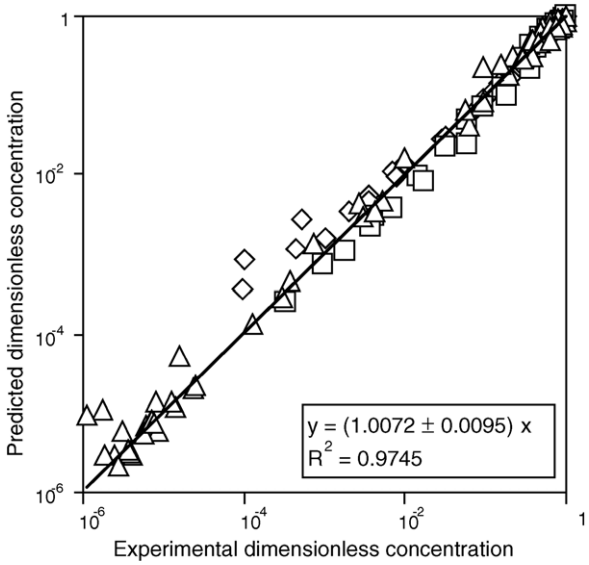

Fig. 10. Bacteria inactivation. Compendium of all experimental data comparing model predictions with experiments: (□) $C_m = 4 \times 10^{-6}$ g cm^{-3} (nutrient broth); (◊) $C_m = 5 \times 10^{-6}$ g cm^{-3} (synthetic broth); (△) $C_m = 1 \times 10^{-3}$ g cm^{-3} (nutrient broth). Runs were made with Heraeus NNI40 and Philips TUV15 lamps and different initial CFU concentrations.

It must be noted that k_G has been obtained from separate experiments measuring the kinetics of bacteria growth employing irradiated, but viable bacteria:

$$k_G = 1.50 \times 10^2 \pm 14.90 \text{ CFU g}^{-1} \text{ s}^{-1}$$

On the other hand, k_{prot} cannot be estimated separately and will be the result of the non-linear, mutiparameter estimation obtained from the comparison of the model predictions with the experimental data. Integration of the set of equations [Eqs. (2)–(7) and (10)] was done with a Runge–Kutta routine of second order for stiff ordinary differential equations and the parameter estimation was performed with a modification of the well-known Levenberg–Marquardt algorithm [28,29]. Parameter estimations were made for different values of n ($n = 0, 1, 2, \ldots, n$). The value of k was taken from the results in diluted media [22]. For each threshold limit the values of k_{prot} and m were estimated. Different initializing values were employed to confirm the uniqueness of the results. For the concentrated medium the following set of parameters was obtained: $n = 2$, $m = 0.205 \pm 0.015$, $k = 9.03 \pm 0.36$ (cm^3 W^{-1})^m s^{-1} or $k = 1.31 \times 10^2 \pm 5.21$ (cm^3 s einstein^{-1})^m s^{-1}, $k_{prot} = 5.46 \times 10^3 \pm 3.39 \times 10^2$ (cm^3 W^{-1})^m cm^3 g^{-1} s^{-1} or $k_{prot} = 7.95 \times 10^4 \pm 4.95 \times 10^3$ (cm^3 s einstein^{-1})^m cm^3 g^{-1} s^{-1}.

Note that the same threshold limit ($n = 2$) and the same reaction order ($m = 0.205$) with respect to the photon absorption rate have been obtained for both concentrated media and that k was fixed as the corresponding value for dilute media. Hence the optimization procedure applied exclusively to k_{prot}, n and m. Fig. 9 shows some typical results. The solid lines are predictions from the model and the diamonds and circles experimental points. These results are of general validity for the employed bacteria and cultures and can be applied to any type of reactor. If the radiation field is not one-dimensional the appropriate RTE must be used [18]. G_w can be measured with different procedures (actinometric or radiometric) or could be estimated from radiation emission models [18]. k_G and k_{prot} depend on the characteristics of the employed medium and will have to be measured with laboratory experiments for each particular application, but the concepts included in the kinetic model are independent of the reactor configuration. It is also clear that for a reactor of different shape or different operating conditions (not well-mixed, continuous, etc.) the corresponding, specific mass balances in terms of the CFU concentrations will have to be derived.

For transparent waters, when $C_m \to 0$, Eq. (10) reduces to the original set represented by Eq. (1) because:

$$R_G = k_G C_m \cong 0, \qquad k_{obs} = k - k_{prot} C_m \cong k \tag{11}$$

The values of n and m in the case of concentrated medium are equal to the ones obtained for the diluted media. It seems possible to obtain a single set of parameters for both operating conditions. Then, the non-linear, multiparameter estimation was repeated including in the evaluation all the runs: those corresponding to dilute and to concentrated media, with different initial concentrations of the CFU and the four different irradiating conditions. The unified set of parameters, within a 95% confidence interval, resulted: $n = 2$, $m = 0.205 \pm 0.015$, $k = 9.03 \pm 0.36$ (cm^3 W^{-1})^m s^{-1} or $k = 1.31 \times 10^2 \pm 5.21$ (cm^3 s einstein^{-1})^m s^{-1}, $k_G = 1.50 \times 10^2 \pm 14.90$ CFU g^{-1} s^{-1}, $k_{prot} = 5.46 \times 10^3 \pm 1.86 \times 10^2$ (cm^3 W^{-1})^m cm^3 g^{-1} s^{-1} or $k_{prot} = 7.95 \times 10^4 \pm 2.72 \times 10^3$ (cm^3 s einstein^{-1})^m cm^3 g^{-1} s^{-1}.

In Fig. 10, the good agreement between model predictions and experimental data is shown including all the data corresponding to dilute and concentrated medium concentrations, different initial CFU concentrations and different irradiation rates. Thus a single set of parameters can be used for both operating conditions. It should be remarked that the model is limited to media without solid particles because when they are present Eq. (9) will certainly be different and scattering effects should be taken into account changing also very drastically the form of Eqs. (2)–(4).

Table 4
Pseudo-quantum yields for bacteria disinfection

Lamp (nominal power in (W))	Medium concentration ($g\,cm^{-3}$)	$\langle e^{a}_{Ec}\rangle_{L_R}$ (quanta $cm^{-3}\,s^{-1}$)	Bacteria concentration ($CFU\,cm^{-3}$)	Pseudo-quantum yield ($UFC\,quanta^{-1}$)
15	1×10^{-3}	4.88×10^{13}	3.1×10^{7}	1.82×10^{-7}
40	1×10^{-3}	1.96×10^{14}	5.0×10^{7}	6.87×10^{-8}
15	5×10^{-6}	8.91×10^{11}	8.3×10^{4}	1.96×10^{-8}
40	5×10^{-6}	2.23×10^{12}	8.9×10^{4}	3.61×10^{-9}

Note the large difference in *E. coli* initial concentration between the two different media (rows 1 and 2 vs. rows 3 and 4).

Very often research in photochemistry resorts to the concept of overall quantum yield to report some sort of efficiency in the use of the applied photons to the pursued objective. It is interesting to know if it is possible to expand this concept to disinfection processes. Essentially, the overall quantum yield has a very simple definition:

$$\frac{\text{time rate of change of the concentration of a given species}}{\text{volumetric rate of photon absorption by the radiation absorbing species}} \tag{12}$$

In the numerator the chosen species could be a reactant or a product. Strictly speaking the definition applies to monochromatic radiation, but it can be also extended to the polychromatic one. The simplest case is its application to a well-mixed batch reactor with monochromatic irradiation. In mathematical terms:

$$\Phi_\lambda = \frac{\langle R_i(\underline{x},t)\rangle_{V_R}}{\langle e^{a}_{\lambda}(\underline{x},t)\rangle_{V_R}} \tag{13}$$

The volume-averaged values are necessary due to the unavoidable spatial distribution of light intensities. This definition is not complete and has some limitations in the interpretation of the obtained results, because the reaction rate also depends on other variables such as the initial concentration of the species *i*, the time when the reaction rate is measured and many other parameters such as temperature, pH, concentration of the catalyst if used, etc. The LVRPA in the denominator is also a function of time dependent concentrations and the order of magnitude of the irradiation rate. Consequently, all these parameters should be stated when a quantum yield is reported. Usually, some of these uncertainties are solved working with values calculated when $t\to 0$; i.e., with initial rates. The units of the quantum yield are quanta per molecule or einstein per mole (an einstein is the energy of one quanta ($h\nu$) multiplied by the Avogadro's number).

Excluding the short initial time lag when the disinfection rate is equal to zero, we propose to calculate the disinfection pseudo-quantum yield according to the following definition:

$$\left[\frac{\text{initial inactivation rate}}{\text{initial volumetric rate of photon absorption by the bacteria}}\right] \tag{14}$$

$$\Phi_{Inact} = \left[\frac{\langle R_{Ec}(x,t)\rangle_{L_R}}{\langle e^{a}_{Ec}(x,t)\rangle_{L_R}}\right]_{t\to 0+\delta} [=] \frac{CFU\,cm^{-3}\,s^{-1}}{quanta\,cm^{-3}\,s^{-1}} \tag{15}$$

where δ is the short induction time when the concentration of *E. coli* remains constant. In the conventional chemical reaction case, one could, in principle, observe a one to one correspondence between an absorbed photon (having one quanta of energy) and a chemical or energetic change in the molecule. With the exception of chain type reactions, the overall quantum yield is usually less or equal to 1. It is clear that a bacterium is not a single chemical species (an atom or a molecule); consequently, it seems quite unlikely that a single photon (even of short wavelength) could inactivate one CFU. Therefore, one should expect very small values for the overall quantum yield. The units of Φ_{Inact} are CFU per quanta. Table 4 shows the values corresponding to two irradiation rates and disinfection reactions with diluted and concentrated media. According to the physical explanation given before, in all cases the calculated pseudo-quantum yields are extremely low. However, it is very important to observe the very significant effect produced by the order dependence ($m = 0.205$) of the local volumetric rate of photon absorption by the bacteria on the reaction rate. Thus, quantum yields are larger for the lower irradiation rates.

8. Conclusions

A kinetic model describing the inactivation rate of *E. coli* bacteria in contaminated waters has been developed. It can be used with almost clear water conditions as well as in concentrated (and nutritious) media. It takes into account the radiant energy effectively absorbed by the bacteria, the possibility of bacteria growing during the inactivation process in a nutritious medium and the existence of some sort of association effects producing some form of bacteria protection observed in concentrated environments. These results reveal that the effect of the absorbed light intensity on the inactivation rate is not directly proportional to the absorbed incident radiation presenting an unusual 0.205 order dependence.

Acknowledgments

The authors acknowledge the received support from Universidad Nacional del Litoral, FONCYT (BID 1201/OC-AR) and CONICET. Thanks are also given to Eng. E. Luciano (Facultad de Ingeniería Química, Food Engineering Department) for his valuable help in developing and conservation of the bacteria culture and to 3M Microbiology Products for supplying part of the used Petrifilm™ plates. The technical assistance of Eng. C. Romani and Mrs. G. Appendino is gratefully appreciated.

References

[1] J. Blanco, S. Malato, C. Estrada, E. Bandala, S. Gelover, T. Leal, Purificación de aguas por fotocatálisis heterogénea: estado del arte, in: M. Blesa (Ed.), Eliminación de Contaminantes por fotocatálisis heterogénea, Red CYTED VIII-G, Cap. 3, Argentina, 2001.

[2] R. Minear, G. Amy (Eds.), Disinfection By-Products in Water Treatment, CRC Lewis Publishers, Florida, USA, 1996.

[3] N. Gray, Drinking Water Quality, Problems and Solution, John Wiley & Sons, Chichester, UK, 1994.

[4] M. Stefan, C. Williamson, UV light-based applications, in: S. Parsons (Ed.), Advanced Oxidation Processes for Water and Wastewater Treatment, IWA Publishing, Cornwall, UK, 2004.

[5] E. Blatchley III, O. Scheible, Ultraviolet disinfection, in: Wastewater Disinfection: Manual of Practice FD-10 (Chapter 7), WEF, Alexandria, 1996.

[6] J. Guerrero, G. Barbosa, Advantages and limitations on processing foods by UV light, Food Sci. Technol. Int. 10 (2004) 137–147.

[7] J. Jagger, Introduction to Research in Ultraviolet Photobiology, Prentice-Hall, Inc., Englewood Cliffs, NJ, 1967.

[8] H. Chick, Investigations of the laws of disinfection, J. Hyg. 8 (1908) 92–158.

[9] B. Severin, Kinetic modeling of microbial inactivation by ultraviolet, Ph.D. Thesis, University of Illinois at Urbana-Champaign, USA, 1982.

[10] B. Oliver, E. Cosgrove, The disinfection of sewage treatment plant effluents using ultraviolet light, Can. J. Chem. Eng. 53 (1975) 170–174.

[11] R. Emerick, F. Loge, D. Thompson, J. Darby, Factors influencing ultraviolet disinfection performance. Part II. Association of coliform bacteria with wastewater particles, Water Environ. Res. 71 (1999) 1178–1187.

[12] R. Qualls, M. Flynn, J. Johnson, The role of suspended particles in ultraviolet disinfection, J. Water Pollut. Contr. Fed. 55 (1983) 1280–1285.

[13] R. Qualls, S. Ossoff, J. Chang, M. Dorfman, C. Dumais, D. Lobe, J. Johnson, Factors controlling sensitivity in ultraviolet disinfection of secondary effluents, J. Water Pollut. Contr. Fed. 57 (1985) 1006–1011.

[14] J. Darby, M. Heath, J. Jacangelo, F. Loge, P. Swaim, G. Tchobanoglous, Comparative efficiencies of chlorination/dechlorination and ultraviolet irradiation, Re 91-WWD-1, Water Environ. Res. Found., Alexandria, VA, 1995.

[15] R. Emerick, J. Darby, Ultraviolet light disinfection of secondary effluents: predicting performance based on water quality parameters, Plan. Des. Oper. Effluent Disinfection Sys. Spec. Conf. Ser., Water Environ. Fed., Whippany, NJ, 1993.

[16] F. Loge, R. Emerick, M. Heath, J. Jacangelo, G. Tchobanoglous, J. Darby, Ultraviolet disinfection of secondary wastewater effluents: prediction of performance and design, Water Environ. Res. 68 (1996) 900–916.

[17] T. Blume, U. Neis, Improved wastewater disinfection by ultrasonic pretreatment, Ultrason. Sonochem. 11 (2004) 333–336.

[18] A. Cassano, C. Martín, R. Brandi, O. Alfano, Photoreactor analysis and design: fundamentals and applications. A Review, Ind. Eng. Chem. Res. 34 (1995) 2155–2201.

[19] F. Loge, R. Emerick, T. Ginn, J. Darby, Association of coliform bacteria with wastewater particles: impact of operational parameters of the activated sludge process, Water Res. 36 (2002) 41–48.

[20] F. Taghipour, Ultraviolet and ionizing radiation for microorganism inactivation, Water Res. 38 (2004) 3940–3948.

[21] R. Emerick, F. Loge, T. Ginn, J. Darby, Modeling the inactivation of coliform bacteria associated with particles, Water Environ. Res. 72 (2000) 432–438.

[22] M. Labas, R. Brandi, C. Martín, A. Cassano, Kinetics of bacteria inactivation employing UV radiation under clear water conditions, Chem. Eng. J., submitted for publication.

[23] O. Alfano, R. Romero, A. Cassano, A cylindrical photo reactor irradiated from the bottom. I. Radiation flux density generated by a tubular source and a parabolic reflector, Chem. Eng. Sci. 40 (1985) 2119–2127.

[24] M. Labas, C. Zalazar, R. Brandi, C. Martín, A. Cassano, Scaling up of a photoreactor for formic acid degradation employing hydrogen peroxide and UV radiation, Helv. Chim. Acta 85 (2002) 82–95.

[25] J. Bailey, D. Ollis, Biochemical Engineering Fundamentals, 2nd ed., McGraw-Hill Book Company, New York, 1986.

[26] C. Martín, O. Alfano, A. Cassano, Decolorization of waters for domestic supply employing UV radiation + hydrogen peroxide, Catal. Today 60 (2000) 119–127.

[27] R. Stanier, E. Adelberg, J. Ingram, The Microbial World, Prentice-Hall, Inc., Englewood Cliffs, NJ, 1976.

[28] K. Levenberg, A method for the solution of certain problems in least squares, Quart. Appl. Math. 2 (1944) 164–168.

[29] D. Marquardt, An algorithm for least-squares estimation of nonlinear parameters, J. Soc. Ind. Appl. Math. 11 (1963) 431–441.